Published in final edited form as:
Medchemcomm. 2012 April 1; 3(4): 480–483. doi:10.1039/C2MD00301E.

A second generation MRI contrast agent for imaging zinc ions *in vivo*

Luis M. De León-Rodríguez[a], **Angelo J. M. Lubag**[b], **Jorge A. López**[a], **Gabriel Andreu-de-Riquer**[a], **José C. Alvarado-Monzón**[a], and **A. Dean Sherry**[b]

[a] Departamento de Química, Universidad de Guanajuato, Cerro de la Venada s/n, Guanajuato, Gto., C.P. 36040, México.

[b] Advanced Imaging Research Center, University of Texas Southwestern Medical Center, 5323 Harry Hines Blvd, Dallas, Texas 75390-9185, USA

Abstract

A Zn^{2+} specific GdDOTA derivative containing two bis-(3-pyrazolyl) units was prepared and characterized. Unlike a previously reported Zn^{2+} binding agent, the new agent binds to human albumin both in the presence and absence of Zn^{2+}.

Magnetic resonance imaging (MRI) contrast agents (CAs) are widely used in clinical practice to measure dynamic processes or to highlight tissue abnormalities. Most current Gd^{3+}-based, T_1 shortening CAs available to clinicians are considered nonspecific, extracellular agents. One exception is the recently approved albumin binding agent, Ablavar,[1] an agent that remains largely confined to the vascular blood pool and hence useful for vascular imaging. Other second generation CAs will likely also display high specificity for biomolecular targets or be responsive to specific biological stimuli (eg. oxidation, metals, enzymes, etc.).[2] CAs responsive to zinc ions (Zn^{2+}) are particularly interesting since imbalances in this ion are related to several pathologies including Alzheimers disease, prostate cancer and diabetes. Brain, prostate and pancreas contain concentrations of $^{Zn2+}$ high enough to make this ion suitable for imaging by MRI in these organs.[3-5] Several Zn^{2+}-responsive CAs have been reported[6-10] but few have been shown to work *in vivo*.[10,11] Among the factors that can limit *in vivo* applications of such sensor for imaging Zn^{2+} include the binding affinity between the CA and Zn^{2+} (K_D) and the proton longitudinal relaxivity (r_1) change that occurs upon binding of Zn^{2+} ions to the CA. It has been proposed that K_D values for any Zn^{2+} MRI specific CA should be in the ~μM range for *in vivo* applications (for single molecule CAs where r_1 changes upon stimuli recognition are limited).[10] One recently reported MRI Zn^{2+} specific CAs that shows promise for imaging beta cell function *in vivo*, GdDOTA-diBPEN, forms a 1:2 complex with Zn^{2+} (one Zn^{2+} per BPEN) with a K_D = 33.6 nM. A particular feature of this agent is that it shows a modest increase (~20%) in r_1 upon binding to Zn^{2+} in the absence of albumin (37 °C, pH 7.6, 0.1 M Tris buffer, 23 MHz), but a substantial change in r_1 (~165% from 6.6 to 17.4 $mM^{-1}s^{-1}$) upon formation of a 1:2 complex with Zn^{2+} ions in the presence of fatty acid free human serum albumin (HSA). This enhanced r_1 results from binding of GdDOTA-diBPEN$(Zn)_2$ to site 2 of the protein with a K_D ~ 45 μM.[10] The r_1 enhancement was more modest (~40%, from 6.1 to 8.6 $mM^{-1}s^{-1}$) when the agent was mixed with human blood plasma, likely reflecting more competition with other serum components for binding to HSA. In an effort to maximize the binding interactions between Zn^{2+} agents like GdDOTA-diBPEN with

Fax: 52 4737326252 lmdeleon@quijote.ugto.mx.

HSA in serum, a simple modification of the Zn^{2+} binding arms was first considered. Given the relatively high affinity of GdDOTA-diBPEN$(Zn)_2$ for site 2 of HSA, a largely hydrophobic binding pocket, it is reasonable to assume that the pyridine groups of ZnBPEN adopt a conformation that favors π-π interactions within the site 2 binding cavity.[10] Any factor that weakens this interaction *in vivo* will have a deleterious affect on the observed r_1. The BPEN moiety and a number of variations have been explored in the design of Zn^{2+} sensors.[12] Here, we describe the synthesis and characterization of a 3-pyrazolyl version of GdDOTA-diBPEN and explore its utility as a Zn^{2+} sensor *in vivo*. The 3-pyrazolyl moiety was chosen because it retains a pyridine-like nitrogen atom (N^2) to act as a donor atom for Zn^{2+} but also has a neighboring N^1H group known to stablize metal ion complexes via added hydrogen bonding interactions.[13] This feature could provide additional stability between the Zn^{2+}-agent and HSA.

A GdDOTA derivative containing two N,N-bis-(3-pyrazolyl-methyl) ethylene diamine (BPYREN) units (GdDOTA-diBPYREN, Fig. 1) was prepared (see Scheme S1, ESI†). The r_1 relaxivity of GdDOTA-diBPYREN increased upon addition of Zn^{2+} and Cu^{2+} but did not change with added Ca^{2+} or Mg^{2+}. The relaxivity of the complex was 4.2 ± 0.1 mM^{-1} s^{-1} (37 °C, pH 7.6, 0.1 M Tris buffer, 23 MHz) in the absence of Zn^{2+} and this gradually increased to 6.9 ± 0.2 mM^{-1} s^{-1} with addition of Zn^{2+} until 2 equiv had been added, remaining constant with 3 equiv of Zn^{2+} (Fig. 2). This is consistent with formation of a 1:2 (Gd:Zn) complex. Mass peaks from GdDOTA-diBPYREN(Zn), adducts of this complex with Na^+ and K^+, and GdDOTA-diBPYREN$(Zn)_2$ were observed by MALDI-TOF MS spectroscopy confirming the formation of 1:2 complex (Gd:Zn) complex (Fig. S6 and S7, ESI†). The r_1 changes upon metal binding were more dramatic for Zn^{2+} than for Cu^{2+}.

Relaxivity changes in presence of HSA were also measured for GdDOTA-diBPYREN. Here, r_1 increased from 8.4 ± 0.2 mM^{-1} s^{-1} in absence of Zn^{2+} (37 °C, pH 7.6, 0.1 M Tris buffer, 0.6 mM HSA, 23 MHz) to 15.3 ± 0.4 mM^{-1} s^{-1} with addition of 3 equiv of Zn^{2+}. The higher r_1 of GdDOTA-diBPYREN in HSA in absence of Zn^{2+} compared to GdDOTA-diBPEN (6.6 ± 0.1 mM^{-1} s^{-1}) suggests that the former might be binding to the protein as well. The relaxivity also increased in similar magnitude to that of Zn^{2+} in presence of Cu^{2+} in HSA buffered solution but remained unchanged with Ca^{2+} and Mg^{2+}. For reference the r_1 of Prohance™ (GdDO3A) a clinically used CA, was determined to be 2.9 ± 0.1 $mM^{-1}s^{-1}$ (37 °C, pH 7.6, 0.1 M Tris buffer with 0.6 mM HSA, 23 MHz) in absence of Zn^{2+} and 2.7 ± 0.1 $mM^{-1}s^{-1}$ with 3 equiv of Zn^{2+}.

An observation made during the T_1 measurements in absence of HSA was that the slight precipitation of Zn^{2+} for solutions containing CA: Zn^{2+} ratios above 1:1, indicating a weak binding of Zn^{2+}, which will precipitate at pH 7.6 in the absence of a chelating ligand.

The K_D of GdDOTA-diBPYREN with Zn^{2+} was determined by a competitive assay using the commercially available fluorophore FluoZin-1 (see ESI†). This dye was chosen since it shows a moderate metal binding. Using the experimentally determined dissociation constant for the dye (24.3 ± 2.8 μM), a binding constant of 378.6 ± 83.1 μM was estimated for formation of GdDOTA-diBPYREN$(Zn)_2$ (per BPYREN binding unit). As expected a much weaker affinity for Zn^{2+} than GdDOTA-diBPEN was found.

Relaxivity measurements were performed in presence of warfarin or dansylsarcosine, which are known to bind HSA at site 1 or 2 respectively. A 18% decrease in r_1 was observed when dansylsarcosine (5 equiv relative to GdDOTA-diBPYREN) was added to a solution

†Electronic Supplementary Information (ESI) available: General experimental conditions, synthesis, relaxometric and fluorescence experiments and MRI details.

containing agent/Zn^{2+} 1/2 in HSA buffered solution, while no change in r_1 was observed upon addition of warfarin under the same conditions. Also a 16% decrease in r_1 was determined when dansylsarcosine was added to GdDOTA-diBPYREN in absence of Zn^{2+} while no change was seen when warfarin was added. These results indicate that both GdDOTA-diBPYREN and GdDOTA-diBPYREN$(Zn)_2$ bind to site 2 of subdomain IIIA of HSA.

To gain further insight into binding of the agent to HSA, a change in water proton relaxation rates (ΔR_1) was measured under conditions where the concentration of HSA was varied while the concentration of GdDOTA-diBPYREN and Zn^{2+} (1:2) or GdDOTA-diBPYREN alone was maintained constant (Fig. 3). For GdDOTA-diBPYREN alone a K_D of 10.7 ± 0.9 μM with HSA was determined (see ESI†). The titration curve of GdDOTA-diBPYREN in the presence of 1:2 $^{Zn2+}$ showed quite a different binding feature. At low concentrations of HSA, ΔR_1 increased in parallel to that observed for Zn^{2+} free GdDOTA-diBPYREN but at higher concentrations of HSA ΔR_1 decreased. To explain this observation one should consider that HSA has a Zn^{2+} binding site with a K_D of 29.5 nM[14] so that the observed behaviour in the titration curve of GdDOTA-diBPYREN with Zn^{2+} shows that HSA is competing for Zn^{2+} with the agent as expected given the weaker binding of BPYREN to Zn^{2+} than HSA.

Fitting the titration curve for HSA < 0.2 M allows one to estimate a K_D of 29.4 ± 2.2 μM GdDOTA-diBPYREN$(Zn)_2$ to HSA, which indicates that the agent reported herein has a stronger binding to HSA than GdDOTA-diBPEN$(Zn)_2$ (K_D ~ 45 μM).[10]

To determine the effectiveness of GdDOTA-diBPYREN as a relaxation agent under physiological conditions, relaxivity measurements were also performed in human blood serum. In this case, r_1 increased from 6.0 ± 0.1 to 13.1 ± 0.1 $mM^{-1}s^{-1}$ (37 °C, 23 MHz) upon addition of Zn^{2+} a 114% change which is ~3 fold larger than that found for GdDOTA-diBPEN. This suggests that the 3-pyrazolyl groups provide added stablility between the Zn^{2+}-bound agent and the protein.

Given the relatively large change in r_1 observed for GdDOTA-diBPYREN in serum, MR images (9.4T) of 24 hr fasted mice were collected before and after glucose stimulated insulin/Zn^{2+} release from pancreas as reported for GdDOTA-diBPEN.[15] Fasting glucose levels were measured in representative animals prior to imaging (~ 5.6 ± 0.3 mM, considered normal). After collection of anatomical multi-slice images to locate the pancreas, each mouse was given a bolus injection of glucose standard intraperitoneally (2 mg/Kg body weight, i.p.) or a saline solution for control mice followed ~10 min later by a bolus of GdDOTA-diBPYREN or Prohance™ (2.5 μmol; 4 times higher than the amount used of GdDOTA-diBPEN) via a tail vein catheter. With this protocol, T_1 weighted images showed a significant enhancement within 10 min after GdDOTA-diBPYREN injection for the animals given a prior bolus of glucose (10 min prior to contrast agent injection) (Fig. 4) which is in agreement to what was previously observed with GdDOTA-diBPEN. This is evidence that GdDOTA-diBPYREN is sensing secretion of Zn^{2+} from β-cells of the pancreas in response to a glucose stimulus. On the other hand, when no glucose was injected (saline injection) the pancreas region showed a quick and significant contrast enhancement in the pancreas area within 5 min after GdDOTA-diBPYREN injection followed by an immediate decrease (Fig. 5 curve with rhombic symbols). This later behaviour corresponds to what is observed with non-specific CAs (Fig. 5 curve with triangle symbols). The relaxivity change in presence of HSA for GdDOTA-diBPYREN at 9.4T (400 MHz) was substantially smaller than the increase observed at 23 MHz, as expected for a complex undergoing slow rotation (r_1 increased from 3.2 ± 0.2 mM^{-1} s^{-1} in absence of Zn^{2+} (37 °C, pH 7.6, 0.1 M Tris buffer, 0.6 mM HSA, 400 MHz) to 4.0 ± 0.3 mM^{-1} s^{-1} with addition of

2 equiv of Zn^{2+}). However, this change is still significant for detection of glucose stimulated Zn^{2+} secretion *in vivo*.

To summarize this work, we report here a new Zn^{2+} MRI agent containing 3-pyrazolyl groups that has a suboptimal binding affinity for Zn^{2+} but has an improved binding interaction with HSA. This agent shows the highest reported r_1 change in human serum upon Zn^{2+} recognition. These results suggest that future designs of Zn^{2+} specific MRI CAs based on the HSA binding principle should consider optimizing interactions between the agent and the protein.

No gating was employed. Each image includes phantoms in capillary tubes positioned horizontally and aligned with the mouse body. These phantoms contain GdDOTA-diBPYREN, 25 μM; H_2O; $GdCl_3$, 25 μM, Prohance™ ; 25 μM clockwise from bottom-left to bottom-right. The yellow arrow points the pancreas location.

Supplementary Material

Refer to Web version on PubMed Central for supplementary material.

Acknowledgments

This research was supported in part by Universidad de Guanajuato (DAIP) Grant 000024/10 and SEP Grant UGTO-CA-107 and by grants from the National Institutes of Health USA (DK-058398 and RR-02584) and Robert A. Welch Foundation Grant AT-584.

References

1. Goyen M. Vasc. Health Risk Manag. 2008; 4:1. [PubMed: 18629367]
2. De Leon-Rodriguez LM, Lubag AJM, Malloy CR, Martinez GV, Gillies RJ, Sherry AD. Acc. Chem. Res. 2009; 42:948. [PubMed: 19265438]
3. Jomova K, Vondrakova D, Lawson M, Valko M. Mol. Cell. Biochem. 2010; 345:91. [PubMed: 20730621]
4. Gumulec J, Masarik M, Krizkova S, Adam V, Hubalek J, Hrabeta J, Eckschlager T, Stiborova M, Kizek R. Curr. Med. Chem. 2011; 18:5041. [PubMed: 22050752]
5. Jansen J, Karges W, Rink L. J. Nutr. Biochem. 2009; 20:399. [PubMed: 19442898]
6. Hanaoka K, Kikuchi K, Urano Y, Nagano T. J. Chem. Soc., Perkin Trans. 2. 2001:1840.
7. Hanaoka K, Kikuchi K, Urano Y, Narazaki M, Yokawa T, Sakamoto S, Yamaguchi K, Nagano T. Chem. Biol. 2002; 9:1027. [PubMed: 12323377]
8. Zhang XA, Lovejoy KS, Jasanoff A, Lippard SJ. P. Natl. Acad. Sci. U.S.A. 2007; 104:10780.
9. Major JL, Parigi G, Luchinat C, Meade TJ. Proc. Natl. Acad. Sci. U. S. A. 2007; 104:13881. [PubMed: 17724345]
10. Esqueda AC, López JA, Andreu-de-Riquer G, Alvarado-Monzón JC, Ratnakar J, Lubag AJM, Sherry AD, De León-Rodríguez LM. J. Am. Chem. Soc. 2009; 131:11387. [PubMed: 19630391]
11. Lee T, Zhang X. a. Dhar S, Faas H, Lippard SJ, Jasanoff A. Chem. Biol. 2010; 17:665. [PubMed: 20609416]
12. Nolan EM, Lippard SJ. Acc. Chem. Res. 2009; 42:193. [PubMed: 18989940]
13. Pérez J, Riera L. Eur. J. Inorg. Chem. 2009:4913.
14. Stewart AJ, Blindauer CA, Berezenko S, Sleep D, Sadler PJ. Proc. Natl. Acad. Sci. U. S. A. 2003; 100:3701. [PubMed: 12598656]
15. Lubag AJM, De Leon-Rodriguez LM, Burgess SC, Sherry AD. P. Natl. Acad. Sci. U.S.A. 2011; 108:18400.

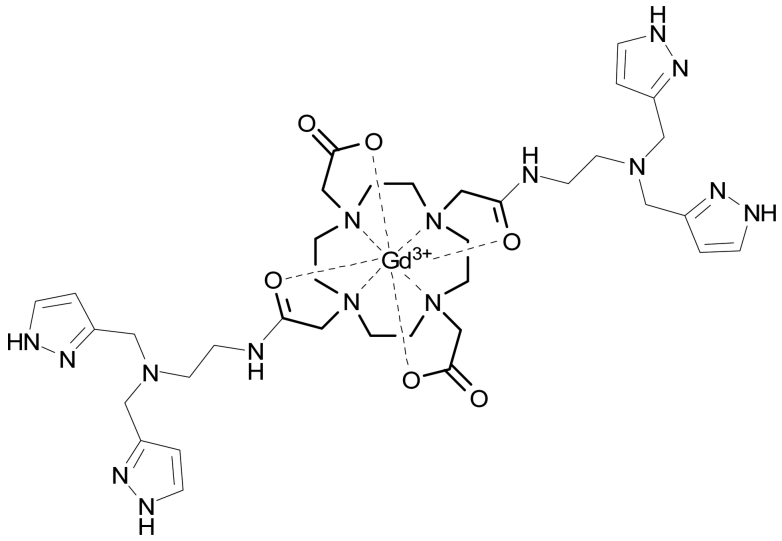

Fig. 1.
GdDOTA-diBPYREN. For the 3-pyrazolyl units the most stable isomer is shown.

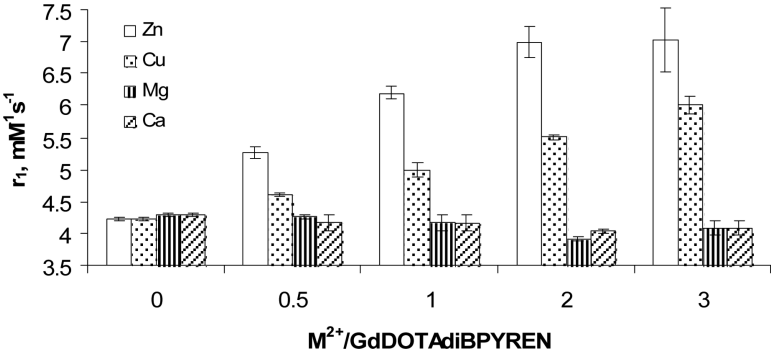

Fig 2.

Relaxivity of GdDOTA-diBPYREN at 23 MHz and 37 °C in the presence of MCl_2, where M = Zn^{2+}, Cu^{2+}, Ca^{2+}, or Mg^{2+}. All solutions were prepared in 100 mM Tris buffer at pH 7.6. r_1 was determined from the slope of the line of the reciprocal of T_1 versus the concentration of gadolinium (GdDOTA- diBPYREN was varied from 1 to 5 mM).

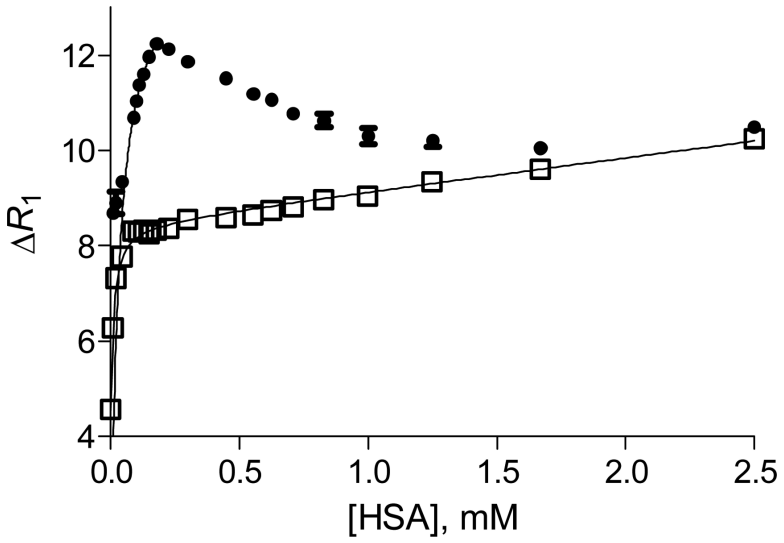

Fig. 3.

Titration of GdDOTA-diBPYREN 1 mM (squares), and GdDOTA-diBPYREN 1 mM plus 2 mM of Zn^{2+} (circles) with HSA. All measurements were made at 23 MHz and 37 °C in 100 mM Tris buffer at pH 7.6. The solid curves represent the best fit to eq 4 in [ESI†].

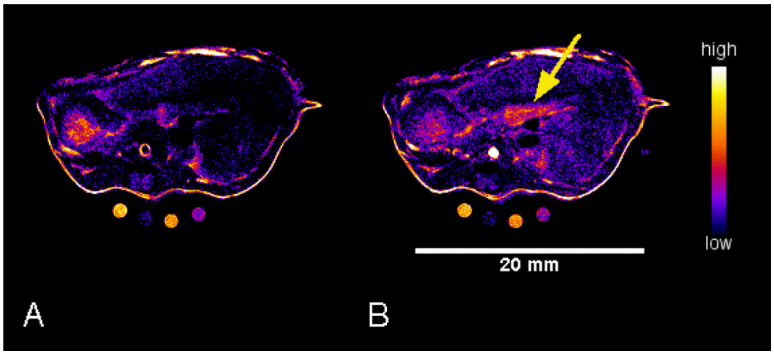

Fig. 4.

T_1-weighted MR images of the mouse abdomen showing the axial view of the pancreas (duodenal side). Pre-GdDOTA-biPYREN (A), and 10 min post i.v. injection of the CA (B). Images were collected using a FSEMS sequence with the following parameters: TR = 89.03 ms; effective echo time (TE) = 11.21 ms; FOV 30×30 mm^2, data matrix = 256×256, averaging = 3, slice = 1 mm, number of slices = 6, gap = 0; ETL=1, kzero = 1.

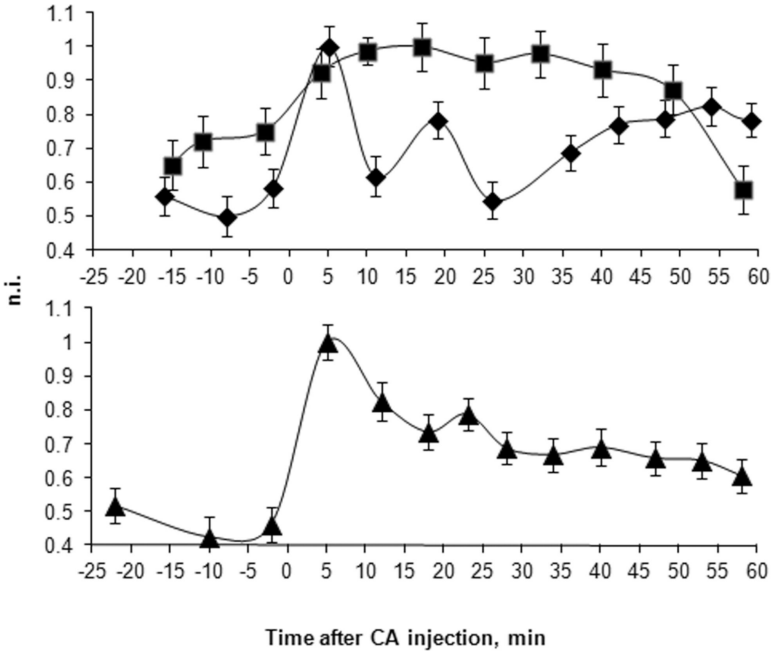

Fig, 5.

Image normalized intensity (n.i.) plot of the duodenal pancreas region. Top graph ■ corresponds to GdDOTA-diBPYREN after i.p. injection of glucose and ◆ corresponds to GdDOTA-diBPYREN after i.p. injection of saline. Bottom graph ▼ corresponds to Prohance™ after i.p. injection of glucose. Image intensity was normalized relative to the highest intensity point for each curve. Agent i.v. injection correspondes to time = 0.